MARINE GEORESOURCES & GEOTECHNOLOGY
http://dx.doi.org/10.1080/1064119X.2016.1213338

Taylor & Francis
Taylor & Francis Group

# Experiment and statistical assessment on piping failures in soils with different gradations

Kuo-Hsin Yang and Jyun-Yen Wang

Department of Civil and Construction Engineering, National Taiwan University of Science and Technology (Taiwan Tech), Taipei, Taiwan

**ABSTRACT**

A series of upward seepage tests on sand specimens with three grain size distributions (i.e., two uniform soils and one gap-graded soil) were conducted to better understand the seepage failure of sea defense systems and coastal hydraulic structures. The objectives were to provide a detailed description of the piping progress and failure mechanism of soils subject to seepage and to investigate the influence of soil gradations on the piping failure modes. In addition, a data set consisting of a wide range of grain size distributions was compiled to assess statistically the accuracy and applicability of critical hydraulic gradient, $i_{cr}$, prediction methods. Experimental results indicated that the piping failure modes of sand specimens depended on soil internal stability, which was related to the grain size distribution. Piping failure of uniform sand, classified as internally stable soil, was associated with an effective stress equal to zero, whereas piping failure of gap-graded sand, classified as internally unstable soil, was caused by the internal erosion of fines. The average $i_{cr}$ values of uniform sand are in good agreement with Terzaghi's theoretical value. However, the average $i_{cr}$ value of gap-graded sand is far lower than Terzaghi's $i_{cr}$ value. The statistical results indicated that Terzaghi's method with Kezdi's internal stability criterion shows the most accurate results with the smallest variance (model bias mean $\mu = 1.04$ and coefficient of variation (COV) = 8.08%) for predicting the $i_{cr}$ of internally stable soils. For internally unstable soils, methods based on the force equilibrium on a soil particle generally produce reasonable μ values ($\mu = 1.20$–$1.75$), but the COV values are considerably high. The discrepancy between the predicted and measured $i_{cr}$ values is discussed. The Results and Discussion in this study provide insightful information for the design, strengthening, and maintenance of coastal waterfront structures against soil piping and erosion.

**ARTICLE HISTORY**
Received 23 April 2016
Accepted 12 July 2016

**KEYWORDS**
Critical hydraulic gradient; internal erosion of fines; soil internal stability; soil piping

## Introduction

Because of the influence of global warming and El Nino in recent decades, the sea level rise has been accelerated in recent years. In addition, the frequency and magnitude of extreme weather events have increased dramatically. In several regions worldwide, sea level rise and extreme weather events have caused severe coastal flood disasters, damaged or destroyed numerous sea defense systems and coastal hydraulic structures (e.g., seawall, revetment, dikes, levee, embankment, and jetty), and subsequently affected millions of people and their properties. As a result, preventing seawater invasion and enhancing the stability of the coastal hydraulic structures have become urgent and challenging issues in coastal protection.

The failures of sea defense systems and coastal hydraulic structures are caused by the impacts from wave forces, storm surge, toe scour, overtopping, and backfill soil piping and erosion. The increased hydraulic head is different as seawater level rise may trigger breaches through internal erosion-related failure mechanisms (Figure 1); as a result, the soil piping and erosion problems in coastal hydraulic structures recently have gained increasing attention (Danka and Zhang 2015). Piping processes are particularly hazardous phenomena and may undermine the strength and stability of the granular skeletons of coastal waterfront structures and their foundation (Rice, Duncan, and Davidson 2007; Rice and Duncan 2010; Danka and Zhang 2015). In Southern Taiwan, during 6–10 August 2009, Typhoon Morakot brought extremely torrential rainfall (which exceeded 2,600 mm in Pingtung County) and caused severe floods in coastal area. In this extreme rainfall event, a total of 6 km of coastal waterfront structures along shoreline experienced either damage or catastrophic failures. Huang, Weng, and Chen (2014) conducted a failure investigation on these hydraulic structures and found that the predominant failure modes involved internal seepage failures inside levees and external sliding failures along foundations. Moreover, past case studies have reported that failures of many waterfront structures were associated with seepage-induced soil piping and erosion (Hagerty 1991a, 1991b; Fell et al. 2003; Richards and Reddy 2007; Xu and Zhang 2009; Zhang, Xu, and Jia 2009; Garner and Fannin 2010; Peng and Zhang 2012).

Piping is a form of seepage erosion and refers to the development of pore channels in porous media through which soil particles are moved. Experimental studies have been conducted to investigate the piping erosion process and failure mechanism in earth embankments (Fleshman and Rice 2014; Sharif et al. 2015). Recent studies have revealed that the initiation and progression phases of soil piping and internal erosion may be classified under four

**CONTACT** Kuo-Hsin Yang khy@mail.ntust.edu.tw Department of Civil and Construction Engineering, National Taiwan University of Science and Technology (Taiwan Tech), No. 43, Sec. 4, Keelung Rd.,Taipei, Taiwan.
Color versions of one or more of the figures in this article can be found online on at www.tandfonline.com/umgt.

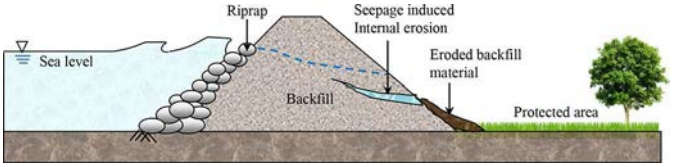


**Figure 1.** Schematic of seepage erosion in coastal hydraulic structures along shoreline due to see level rise.

mechanisms: (1) suffusion, (2) backward erosion, (3) contact erosion, and (4) concentrated leak erosion (Fry 2012; Fell and Fry 2013). This paper focuses on the characteristics and failure progressions of suffusion and backward erosion. *Suffusion* describes the erosion phenomenon in which seepage flows move fine particles through a matrix of coarse soil particles, whereas *backward erosion* denotes the transportation of sand grains with seepage at a free exit surface on the downstream side of a hydraulic structure, causing the development of shallow pipes in the upstream direction. Backward erosion often occurs in the permeable foundations beneath hydraulic structures and causes sand boils or quicksand near the exit because increased pore water pressures produce an effective stress equal to zero.

Many studies have demonstrated that the internal stability of soil and the hydromechanical conditions (i.e., soil stress, seepage direction, and hydraulic gradient) governs the aforementioned soil piping mechanisms (Kenney and Lau 1985; Skempton and Brogan 1994, 1995; Bendahmane, Marot, and Alexis 2008; Ahlinhan and Achmus 2010; Moffat and Fannin 2011a, 2011b; Ke and Takahashi 2012, 2014; Adams, Xiao, and Wright 2013; Chang and Zhang 2013a). The term *internal stability* refers to the ability of a granular material to prevent loss of its own small particles caused by disturbing agents such as seepage and vibration; it is related to soil grain size distribution and its density (Kenney and Lau 1985). Various empirical criteria have been developed for evaluating a soil's internal stability potential (Istomina 1957; Kezdi 1979; Kenney and Lau 1985, 1986; Mao 2005; Wan and Fell 2008; Indraratna, Nguyen, and Rujikiatkamjorn 2011; Chang and Zhang 2011a, 2013b; Li and Fannin 2012, 2013). Table 1 summarizes the three internal stability criteria (Istomina 1957; Kezdi 1979; Kenney and Lau 1985, 1986) that are widely used in design specifications and by researchers to assess the internal stability of cohesionless soil (Skempton and Brogan 1994; Li and Fannin 2008; Wan and Fell 2008; Chang and Zhang 2011b, 2013b). Kezdi's and Kenny and Lau's criteria were adopted in this study and are discussed later.

**Table 1.** Summary of soil internal stability criteria.

| Reference | Internal stability criteria |
|---|---|
| Istomina (1979)[a] | $C_u \leq 10$, internally stable |
| | $10 < C_u < 20$, transitional |
| | $C_u \geq 20$, internally unstable |
| Kezdi (1979)[b] | $(d_{15c}/d_{85f})_{max} \leq 4$, internally stable |
| Kenney and Lau (1985, 1986)[c] | 1985: $(H/F)_{min} > 1.3$, internally stable (original) |
| | 1986: $(H/F)_{min} > 1.0$, internally stable (modified) |

[a] $C_u$ is soil uniformity coefficient obtained from the grain size distribution curve.
[b] $d_{15c}$ is the particle size at finer percent of 15% in coarser fraction and $d_{85f}$ is the particle size at finer percent of 85% in finer fraction.
[c] $F$ is the finer percent at an arbitrary particle diameter $d$; $H$ is the finer percent increment between $d$ and $4d$.

The critical hydraulic gradient $i_{cr}$ values of internally stable soil are close to that predicted using Terzaghi's theoretical equation (Eq. 1) (Terzaghi 1943), which predicts a critical gradient of approximately 1.0; however, for internally unstable soil, the $i_{cr}$ value can be approximately one-fifth to one-third of the theoretical value (Skempton and Brogan 1994).

$$i_{cr} = (G_s - 1)(1 - n) = \frac{\gamma'}{\gamma_w} \quad (1)$$

where $G_s$ is the specific gravity of soil solids; $n$ is the porosity of soil; $\gamma'$ is the submerged unit weight of soil; and $\gamma_w$ is the water unit weight. Equation (1) was developed from the concept that upward seepage force reduces the effective stress in soil to zero. In addition to Terzaghi's theoretical equation, various models have been proposed for determining the $i_{cr}$ for soil piping, including methods based on the force equilibrium on single soil particles (Wu 1980; Liu 1992; Indraratna and Radampola 2002; Mao, Duan, and Wu 2009; Zhou, Bai, and Yao 2010), capillarity and dispersion of clay (Khilar, Folger, and Gray 1985), momentum balance (Moffat and Herrera 2015), and head loss models with porosity and critical velocity concepts (Ojha, Singh, and Adrian 2003). Although these models provide useful tools for predicting when soil piping occurs, studies examining the accuracy of $i_{cr}$ prediction methods are still relatively limited.

This study had three objectives: (1) to provide a detailed description of the failure progress and mechanisms in soils subject to seepage; (2) to investigate the influence of soil gradations on piping failure modes; and (3) to assess statistically the accuracy and applicability of $i_{cr}$ prediction methods reported in the literature. In this study, a series of upward seepage tests on sand specimens with three grain size distributions (i.e., two uniform soil and one gap-graded soils) were conducted. Piping progress and failure mechanisms observed from the tests are described in detail. Furthermore, a data set consisting of a wide variety of grain size distributions was compiled and analyzed. In the context of the data set, $i_{cr}$ prediction methods were examined and their accuracies were statistically assessed and compared. The Results and Discussion in this study provide insightful information for the design, strengthening, and maintenance of coastal waterfront structures against soil piping and erosion.

## Experimental study

### Test system

An upward seepage test system, consisting of a constant head device, a permeameter, and a data acquisition (DAQ) system, was developed in this study (Figure 2). The constant head device contains an elevated water supply reservoir and water barrel positioned at a lower elevation. The water reservoir was connected to the permeameter by a pipe of 1.5 cm in diameter that provided a steady water flow to the soil specimen. To maintain a constant head, an overflow device with a free discharge board was constructed inside the water supply reservoir (Figure 2b). A pump with maximum capacity of 40 L/min was placed inside the barrel to redirect water back to the water supply reservoir. The overflow device and pump

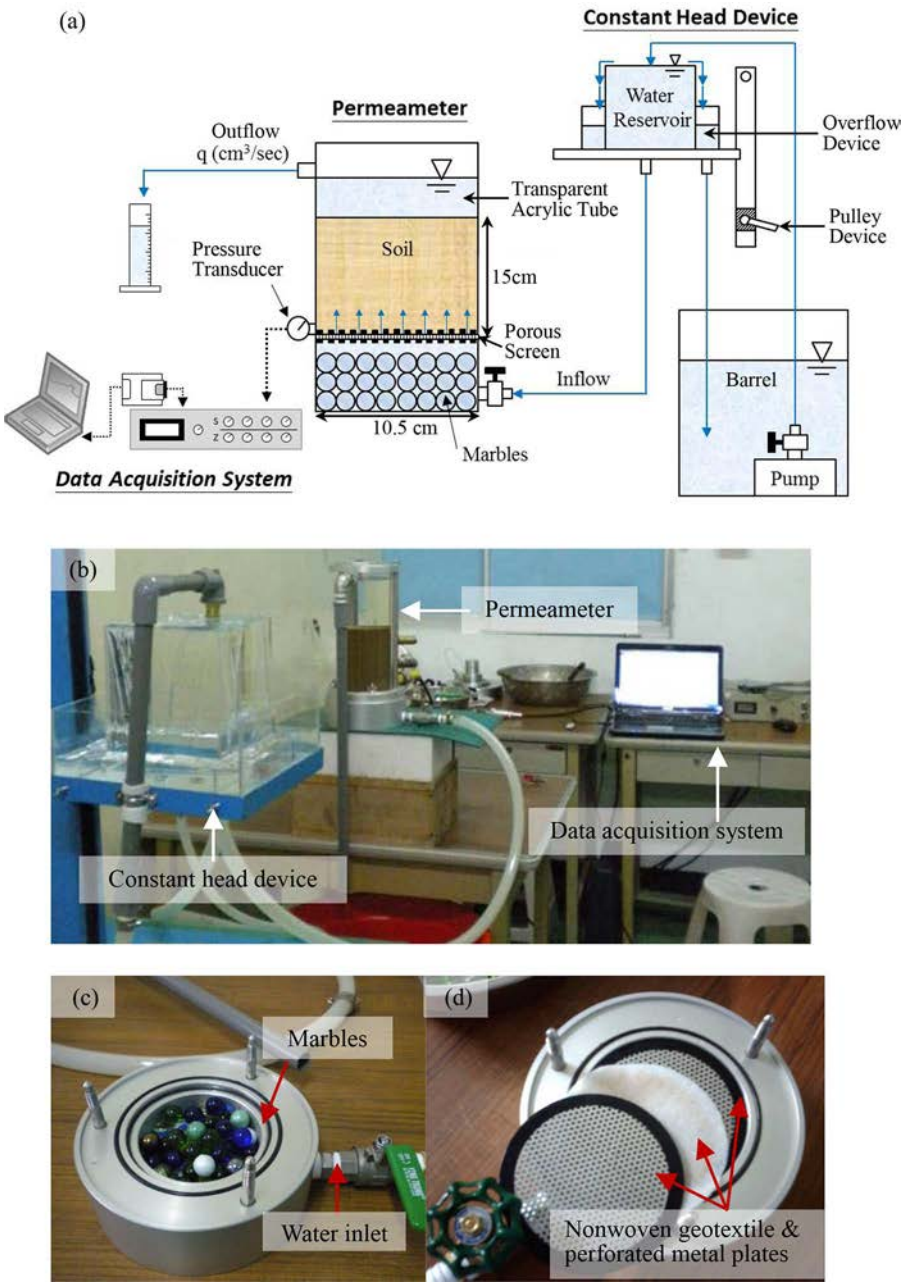


**Figure 2.** Upward seepage test system: (a) Schematic illustration; (b) overview photo of test apparatus: (c) permeameter pedestal filled with marbles; (d) porous screen.

enabled the water to move in a closed loop, which created an automatic water recycling system. The elevation of the water reservoir could be adjusted using a pulley device; positioning the water reservoir at various heights yielded different values of the hydraulic head for tests.

The permeameter consists of a cylindrical cell (10.5 cm in diameter and 38 cm in height) and a bottom pedestal. The cylindrical cell was composed of transparent acrylic, enabling visual observations of seepage and piping progress in soil specimens during tests. The pedestal, filled with marbles and covered by porous screens (Figure 2c, d), was used to distribute the upward seepage evenly across the soil specimen. The marbles were used to minimize the high-pressure water jet effect from the elevated water reservoir. The porous screens comprised two perforated metal plates and a nonwoven geotextile. The perforated metal plates, with many punched holes, were used to support the overburden pressure from soil specimens. The nonwoven geotextile was placed between the two perforated metal plates and served as a filter to prevent the loss of soil. The nonwoven geotextile was carefully selected, so that the hydraulic conductivity of the nonwoven geotextile was much greater than that of the test soil.

The water flow from the top of the specimen was measured and then discharged to the barrel. Discharge velocity $v$ at a given hydraulic gradient was calculated by dividing the collected volume of discharge at a certain time period by the cross-sectional area of the soil specimen. A pressure transducer was inserted at the bottom of each soil specimen to measure the influx water pressure, which was recorded and output in real time through a DAQ system comprising a National

Instruments (NI) USB-9210 DAQ device and NI LabVIEW. The monitored water pressure was used to calculate the corresponding hydraulic gradient applied to the soil specimen.

## Soil properties and specimen preparation

Three soils, Fu-Long beach sand, uniform quartz sand, and gap-graded sand, were tested to investigate the influence of soil gradation on piping failure modes and the associated critical hydraulic gradients. Gap-graded sand is a mixture of 15% Fu-Long sand and 85% coarse sand by dry weight. Fu-Long sand, quartz sand, and gap-graded sand have mean particle size $d_{50}$ values of 0.28, 1.17, and 3.71 mm, respectively. Figure 3 presents the grain size distribution curves of test soils. To avoid scale effect, the ratios of the specimen diameter to the mean grain diameter for Fu-Long sand, Quartz sand, and Gap-graded sands are 375, 90, and 28, respectively. These values are larger than the values (=8–12) specified in ASTM (ASTM D2434). In addition, the diameter of the specimen (i.e., 10.5 cm) also satisfies the ASTM requirement (i.e., cylinder diameter > 7.6 cm) with respect to the grain sizes of the three used soils.

Table 2 summarizes the properties of the selected soils. All test soils are classified as poorly graded sand (SP) according to the Unified Soil Classification System. Uniform Fu-Long sand and quartz sand are also classified as internally stable soils, and gap-graded sand is an internally unstable soil, according to Kezdi's (1979) and Kenny and Lau's (1986) internal stability criteria (Table 2).

Each specimen was carefully prepared to ensure that its soil had a uniform density and full saturation. First, the permeameter was filled with water to a depth of 20 cm at a low flow rate to prevent the generation of air bubbles. Subsequently, the soil specimen was introduced into the permeameter by sedimentation through a 20-cm-deep water column. To achieve the target relative density, $D_r = 70\%$, the soil was filled in six layers (each layer was 2.5 cm thick) and

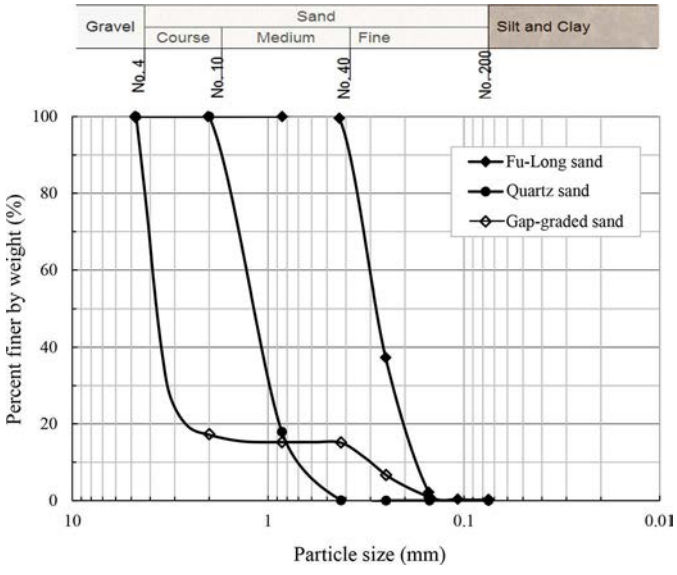


Figure 3. Grain size distribution curves of test soils.

Table 2. Properties of test soil and test conditions.

| Test series | B | C | G |
|---|---|---|---|
| Soil type | Fu-Long sand | Quartz sand | Gap-graded sand |
| Property | | | |
| Mean particle size $d_{50}$ (mm) | 0.28 | 1.17 | 3.71 |
| Uniformity coefficient $C_u$ | 1.72 | 1.77 | 12.7 |
| Coefficient of gradation $C_c$ | 1.01 | 1.03 | 8.82 |
| Specific gravity $G_s$ | 2.65 | 2.65 | 2.65 |
| Soil classification (USCS) | | SP | |
| Max. void ratio $e_{max}$ | 1.01 | 0.86 | 0.92 |
| Min. void ratio $e_{min}$ | 0.59 | 0.63 | 0.55 |
| Avg. hydraulic conductivity $k$ (cm/s) | 0.05 | 0.7 | 1 |
| Internal stability criteria | | | |
| Kezdi (1979) $(d_{15c}/d_{85f})_{max}$ | 1.28 (stable) | 1.44 (stable) | 11.92 (unstable) |
| Kenney and Lau (1986) $(H/F)_{min}$ | 2.07 (stable) | 4.43 (stable) | 0.11 (unstable) |
| Test condition | | | |
| Relative density $D_r$ (%) | 70 | 70 | 70 |
| Porosity $n$ | 0.42 | 0.41 | 0.40 |
| Sample thickness (cm) | 15 | 15 | 15 |
| No. of test | 5 | 5 | 5 |

the required weight of dry soil was determined using the relative density equation:

$$D_r = \frac{(e_{max} - e)}{(e_{max} - e_{min})} \quad (2)$$

where $e_{max}$, $e_{min}$, and $e$ are the maximum, minimum, and target void ratios of soil. A known quantity of dry soil was carefully placed into the permeameter by slowly spreading a scoopful of soil from the periphery to the center of the permeameter. For the gap-graded soils, each soil sample was mixed with water to avoid grain segregation before it was spread into the permeameter. Each layer was slightly compacted using a metal rod to control its height. After each layer had been compacted and leveled, and before the next layer was added, the soil surface was scarified to prepare it for favorable interface bonding with the overlying soil. This procedure was repeated until the desired specimen height (i.e., 15 cm) was reached.

## Test program and procedures

After each specimen had been prepared, it was subject to upward seepage until piping failure occurred. Over the course of the test, the applied hydraulic gradient was incrementally increased; each applied hydraulic gradient was maintained for at least 10 min, so that equilibrium could be reached. The applied hydraulic gradient increment for uniform sand was in the range from $\Delta i = 0.1$ to 0.2 for $i < 0.8$ and $\Delta i = 0.05$ to 0.1 for $i \geq 0.8$. The applied hydraulic gradient increment was set in the range from $\Delta i = 0.05$ to 0.1 for gap-graded sand because the piping failure of gap-graded sand could occur at much smaller $i$ than the uniform sand did. The hydraulic gradient $i$ and corresponding discharge velocity $v$ were recorded in each stage of the test. The repeatability and consistency of the test results were carefully examined by conducting five tests under the same conditions.

## Results and discussion

In this section, test results are presented in $i$–$v$ relationships for each soil type (Figure 4). The piping progress and failure mechanisms of soils subject to seepage are described comprehensively and quantitatively. Moreover, $i$ and $v$ plots were used to determine the onset of piping failure and the associated $i_{cr}$ values of soils with different gradations. The measured $i_{cr}$ values are compared with those predicted using various empirical models, as discussed later.

### *Fu-Long sand*

The measured $i_{cr}$ values of Fu-Long sand vary from 0.93 to 1.05 with an average value of 0.98 (Table 3). The average $i_{cr}$ value agrees with the $i_{cr} = 0.96$ predicted using Terzaghi's theoretical equation. Figure 5 shows a plot of a typical $i$–$v$ relationship from Test B4. Figure 6 shows photographs of piping failures. Details of the piping process are discussed as follows:

(a) At Stages 0–6 ($i = 0$–$0.68$), the $v$ values increase linearly with $i$. The flow is laminar and the hydraulic conductivity $k$ can be obtained according to Darcy's law (i.e., $v = ki$). No noticeable change was detected in the volume of the specimen.

(b) At Stage 7 ($i = 0.81$), a small expansion of 0.2 cm was observed in the specimen.

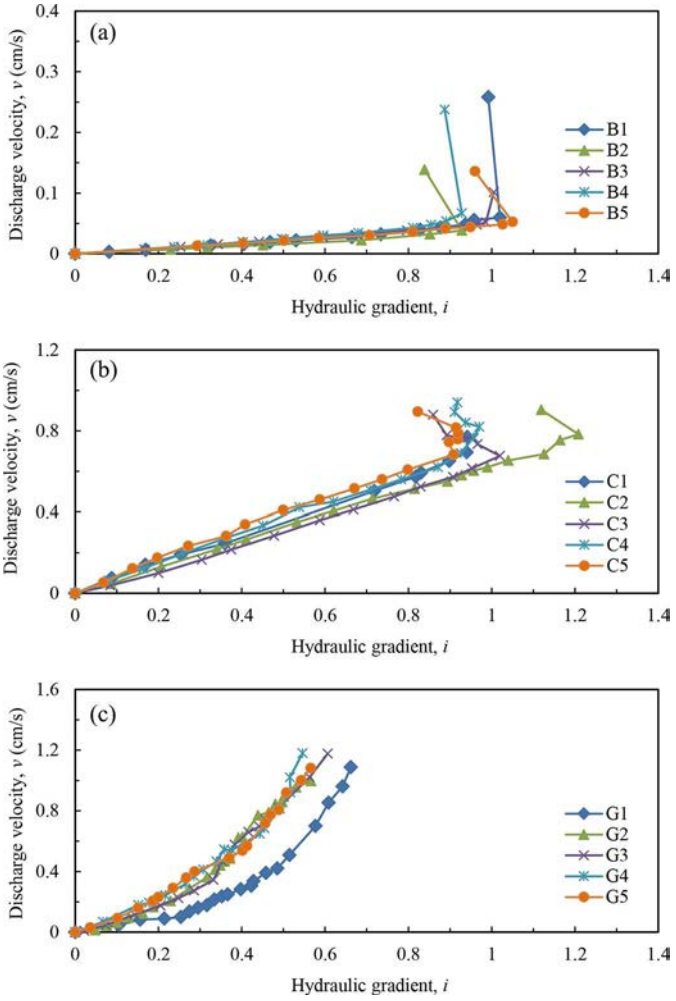


Figure 4. Test results: (a) Fu-Long sand; (b) quartz sand; and (c) gap-graded sand.

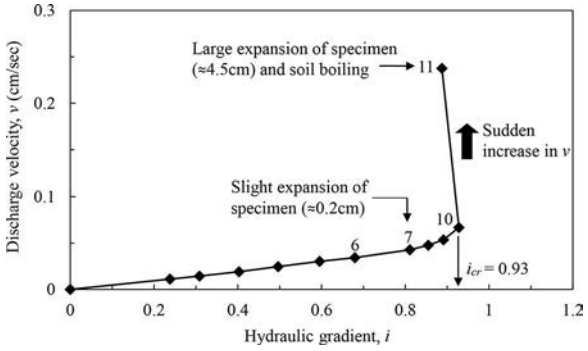


Figure 5. Test B4 result of Fu-Long sand.

(c) At Stage 10 ($i = 0.93$), the expansion of the specimen (≈0.4 cm) became apparent. The $i_{cr}$ of uniform sand was defined at this seepage stage beyond which the discharge velocity in a $v$–$i$ curve increased significantly, indicating that the piping failure occurred (Figure 5); accordingly, the critical hydraulic gradient was determined to be $i_{cr} = 0.93$.

(d) At Stage 11 ($i = 0.89$), the specimen expanded notably (≈4.5 cm) (Figure 6). At this moment, the soil specimen seemed to have liquefied and to have lost its overall stability. Figure 6b shows the formation of a channel; soil was forced to migrate with the upward seepage within the piping channel. Figure 6c shows a close view of vigorous soil

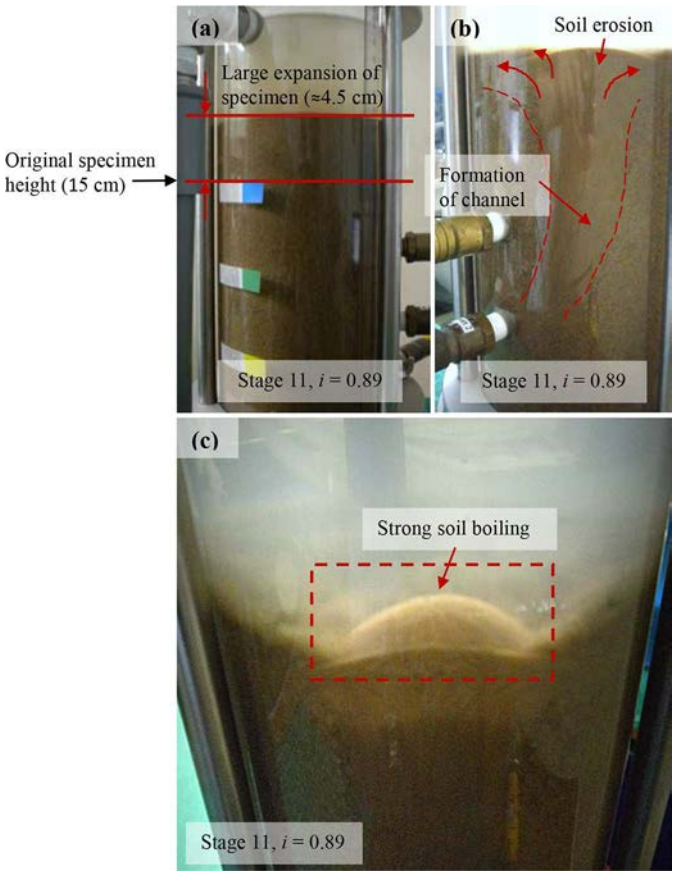


Figure 6. Piping failure of Test B4: (a) large expansion of specimen; (b) washout of soil along a channel; (c) soil erosion and boiling.

**Table 3.** Summary of measured $i_{cr}$ and predicted $i_{cr}$ by Terzaghi's equation.

| Test series | Measured $i_{cr}$ (five test results) | | | | | Avg. of measured $i_{cr}$ | Predicted $i_{cr} = (G_s - 1)(1 - n)$ |
|---|---|---|---|---|---|---|---|
| | 1 | 2 | 3 | 4 | 5 | | |
| B | 1.02 | 0.93 | 0.99 | 0.93 | 1.05 | 0.98 | 0.96 |
| C | 0.94 | 1.21 | 1.02 | 0.97 | 0.92 | 1.01 | 0.97 |
| G | 0.44 | 0.24 | 0.27 | 0.42 | 0.35 | 0.34 | 0.99 |

boil formation on top of the specimen. The measured hydraulic gradient decreased from 0.93 to 0.89 at this stage, although the system total head was increased by elevating the upper water reservoir. The drop of the hydraulic gradient suggests the relief of accumulated pore water pressure within specimens after the piping failure. The pressure drop was also observed in experimental and field tests (Nichols, Sparks, and Wilson 1994; Parekh et al. 2016). The cause of the hydraulic gradient drop is also likely due to the changes of seepage and water pressure conditions which probably transformed from uniform conditions to concentrated flow within the piping channel, as shown in Figure 6b. The pressure transducer, attached to the wall of the cylindrical cell, could not effectively register any pressure changes inside the piping channel. Consequently, the water pressure (or hydraulic gradient) measured at this stage cannot represent the real nonuniform hydraulic conditions across the specimen, particularly the hydraulic conditions within the piping channel.

### Quartz sand

Quartz sand has a grain size distribution curve parallel to that of Fu-Long sand but larger particle sizes. The measured $i_{cr}$ values of quartz sand vary from 0.92 to 1.21 with an average value of 1.01, which is close to the $i_{cr} = 0.97$ predicted using Terzaghi's theoretical equation (Table 3). The test results are shown in Figures 7 and 8. The following observations were made:

(a) At Stages 0–11 ($i = 0$–$0.95$), the measured values of $v$ and $i$ showed a linear relationship, indicating that the soil specimen remained stable in this range of hydraulic gradients.
(b) At Stage 12 ($i = 1.02$), the specimen exhibited a slight expansion (≈0.2 cm). The critical hydraulic gradient was determined at this stage (i.e., $i_{cr} = 1.02$) because the measured $i$ beyond this stage tends to decrease as an indication of the onset of soil piping, as discussed previously.

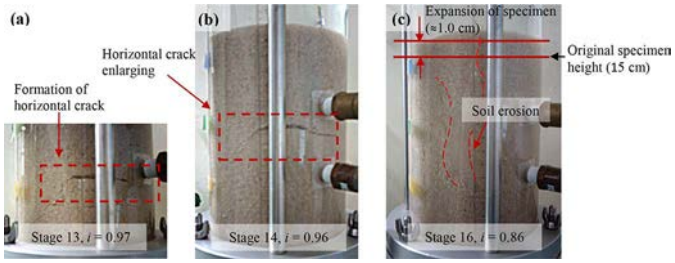


**Figure 8.** Piping failure of Test C3: (a) formation of horizontal crack near specimen bottom; (b) horizontal crack enlarging and rising up; (c) soil erosion with seepage.

(c) At Stage 13 ($i = 0.97$), a visible horizontal crack was formed near the bottom of the specimen (Figure 8a). The decreased $i$ at this stage is likely attributed to the dissipation of accumulated water pressure through the observed horizontal crack. The development of horizontal cracks was also observed by Skempton and Brogan (1994) in their tests on sand specimens with similar porosity.
(d) At Stages 14–16 ($i = 0.96$–$0.86$), the horizontal crack enlarged and moved toward the top of the specimen (Figure 8b). Once the horizontal crack broke through the top of the specimen, soil erosion with seepage and soil heave (≈ 1.0 cm) were observed.

### Gap-graded sand

Gap-graded sand exhibits a distinct gap from 0.4 to 2 mm in its grain size distribution curve and is classified as internally unstable soil according to Kezdi's (1979) and Kenney and Lau's (1986) internal stability criteria (Table 2). The measured $i_{cr}$ values vary from 0.44 to 0.24 with an average value of 0.34, which is much lower than the $i_{cr} = 0.99$ predicted using Terzaghi's theoretical equation (Table 3). In the test (Figures 9 and 10), the following stages of piping development were observed:

(a) At Stages 0–9 ($i = 0$–$0.37$), the measured $v$ increased linearly with increasing $i$. No noteworthy changes in the specimen were detected.
(b) At Stages 10–12 ($i = 0.4$–$0.46$), fine particles exhibited small, jittering movements at the sides of the specimen. Fine particles were gradually eroded out with seepage and remained on the top surface of the specimen.

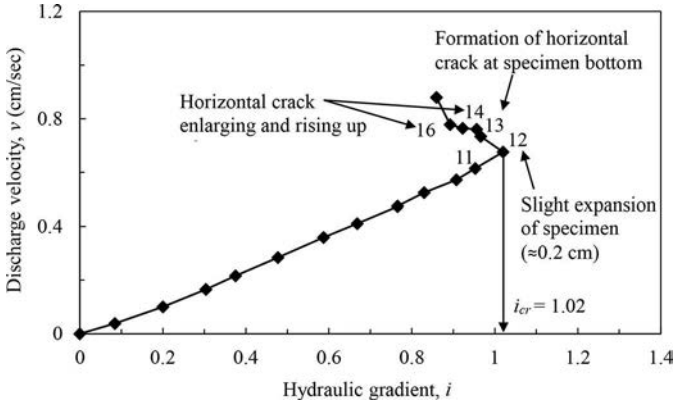


**Figure 7.** Test C3 result of quartz sand.

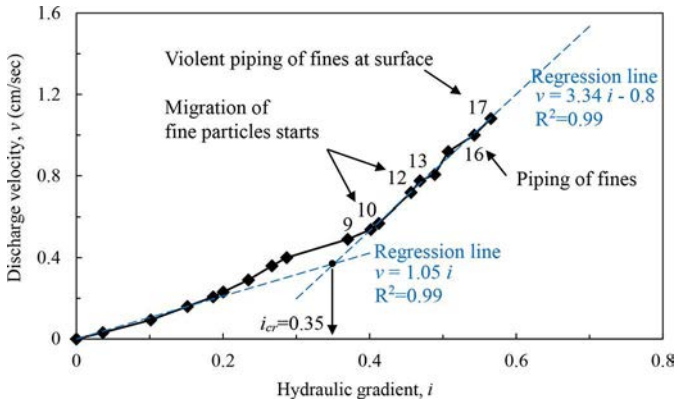


**Figure 9.** Test G5 result of gap-graded sand.

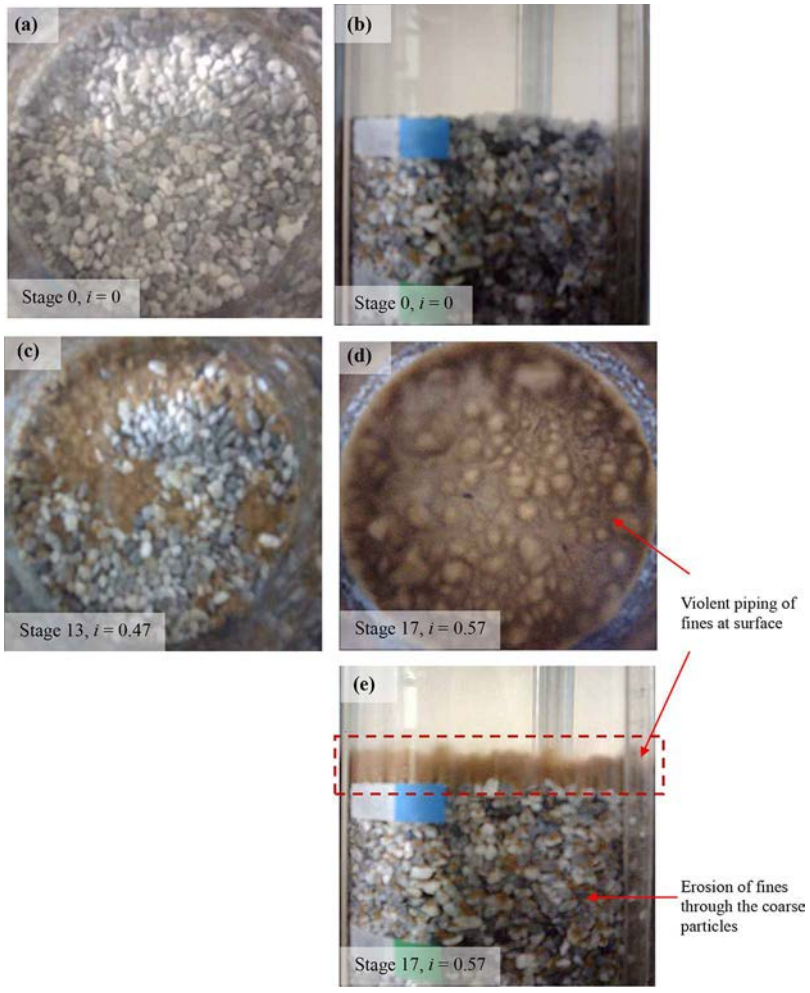


**Figure 10.** Piping failure of Test G5: (a) and (b) before test ($i = 0$); (c) local piping of fines at the top; (d) and (e) violent piping of fines occurred at top (brown part) ($i = 0.57$) and coarse particles remained stable (gray part).

(c) At Stage 13 ($i = 0.47$), slight and local piping of fine particles was observed at the top surface (Figure 10c).
(d) At Stage 16 ($i = 0.54$), piping of fine particles becomes general and washed-out fine particles covered the top surface of the specimen.
(e) At Stage 17 ($i = 0.57$), violent piping of fine particles was observed (Figure 10d, e). Fine particles were largely eroded through seepage, but the coarse particles remained stable, which indicated that the primary framework of coarse particles at this hydraulic gradient was not affected. This process is referred to as segregation piping.

Unlike the i–v curves of Fu-Long sand or quartz sand, those of gap-graded sand did not show an apparent turning point (i.e., a point at which the measured velocity suddenly increases or the hydraulic gradient decreases). To avoid subjectivity in the determination of $i_{cr}$, the $i_{cr}$ for gap-graded sand was determined consistently using a numerical approach at the cross point of two regression lines (Figure 9). As shown in Table 4, the $i_{cr}$ calculated using this approach, on average ($i_{cr} = 0.34$), was close to the average $i_{cr} = 0.38$ observed at the onset of fine particle erosion. The hydraulic conductivity (slope of the regression line) before $i_{cr}$ is $k = 1.05$ cm/s; it increases to $k = 3.34$ cm/s after $i_{cr}$ because of increased soil porosity caused by the erosion of fine particles from the voids among coarse particles.

## Summary and discussion

According to the experimental observations, internally stable soils (i.e., Fu-Long sand and quartz sand) failed through either the general expansion of the soil specimen or the opening of a horizontal crack around or below mid-depth that then moved

**Table 4.** Determination of $i_{cr}$ of gap-graded sand.

| Test series: G (gap-graded sand) | | Test no. 1 | 2 | 3 | 4 | 5 | Average |
|---|---|---|---|---|---|---|---|
| Measured $i_{cr}$ | Mathematic: cross point of regression lines | 0.44 | 0.24 | 0.27 | 0.42 | 0.35 | 0.34 |
| | Observation: onset of finer particle begin to move | 0.40 | 0.37 | 0.35 | 0.38 | 0.40 | 0.38 |
| | Observation: violent piping of fines | 0.64 | 0.53 | 0.60 | 0.55 | 0.57 | 0.57 |

to the top. When piping broke through these specimens, the soils were vigorously eroded and migrated with the upward seepage within the piping channels. In addition, the hydraulic gradient decreased when piping failures occurred because of the nonuniform hydraulic conditions across the specimens. The internally unstable soil (i.e., gap-graded sand) failed through erosion of fine particles through the voids of a framework formed predominately of coarse particles. The test results confirm Kezdi's and Kenney and Lau's criteria for the internal stability of granular materials. Furthermore, Terzaghi's $i_{cr}$ equation can generate an accurate prediction result for internally stable sands but tended to overestimate the $i_{cr}$ for internally unstable soil in this study.

Vertical effective stress $\sigma_v'$ for a specimen subject to upward seepage is evaluated as

$$\sigma_v' = (\gamma_{sat} - \gamma_w)z - i \cdot z \cdot \gamma_w \tag{3}$$

where $\gamma_{sat}$ is the saturated unit weight of soil; $\gamma_w$ is the unit weight of water; $i$ is the hydraulic gradient ($i = i_{cr}$ at soil piping failure); and $z$ is the specimen height (15 cm). The calculated $\sigma_v'$ values for Fu-Long sand and quartz sand at $i_{cr}$ (Figure 11) are close to zero, suggesting that the soil submerged weight is counterbalanced by the upward seepage force. Consequently, as observed in the tests, soils were liquefied and lost overall stability at piping failure. This $\sigma_v' = 0$ condition is consistent with the theoretical background of Terzaghi's $i_{cr}$ equation. Therefore, Terzaghi's equation can predict the $i_{cr}$ of uniform sand accurately. By contrast, Figure 11 shows $\sigma_v' > 0$ for gap-graded sand at piping failure. As observed in the tests, the fine particles were washed out at soil piping failure, but the coarse particles of the gap-graded sand remained comparatively stable. Terzaghi's $i_{cr}$ theoretical background differs from the aforementioned condition and Terzaghi's theory thus does not predict the $i_{cr}$ of gap-graded soil correctly.

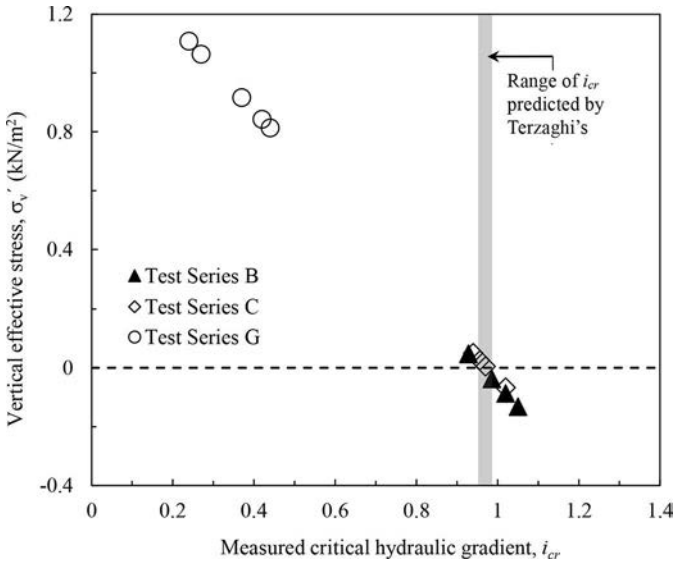


Figure 11. Soil effective stress states at critical hydraulic gradient.

## Statistical assessment of $i_{cr}$ prediction

A data set consisting of a total of 44 test data from Skempton and Brogan (1994), Mörz et al. (2007), Mao, Duan, and Wu (2009), Ahlinhan and Achmus (2010), Ke and Takahashi (2011), and this study was compiled and analyzed to assess the statistical accuracy and applicability of $i_{cr}$ prediction methods reported in the literature. The compiled soil specimens consisted of sand and sandy gravel with a wide range of grain size distributions. Table 5 describes statistical attributes of the compiled piping test data set.

### $i_{cr}$ prediction methods

In addition to Terzaghi's theoretical equation (Eq. 1), various theoretical and empirical models have been proposed for determining the $i_{cr}$ for soil piping, as discussed in the Introduction section. Among these models, three models based on the force equilibrium on a single soil particle (Wu 1980; Liu 1992; Zhou, Bai, and Yao 2010) were selected for the analyses in this study. Figure 12 illustrates the force components considered in Zhou's force equilibrium model. These models estimate the $i_{cr}$ at the onset of fine particle motion, which can better represent the piping failure mode of internally unstable soils. Table 6 summarizes the $i_{cr}$ prediction methods used in this study. The theoretical backgrounds of these methods are introduced in the following section. Input parameters for these methods are listed in Table 5.

### Wu (1980)

Wu (1980) proposed a model for calculating the critical hydraulic gradient of soil based on the equilibrium of frictional force and dynamic pressure of flowing water acting on a soil particle. Wu's $i_{cr}$ equation is expressed as

$$i_{cr} = (G_s - 1)\frac{d_f}{d_f + e d_{eq}} \tag{4}$$

where $G_s$ is the specific gravity of soil solids; $e$ is the void ratio of soil (which can be derived from porosity $n$ using the volume–weight relationships of soil); $d_f$ is the particle diameter of the eroded soil, which is assumed to be the effective soil particle size $d_{10}$; and $d_{eq}$ is the equivalent particle diameter, calculated as

$$d_{eq} = \frac{100\%}{\sum(f_i / d_{ave,i})} \tag{5}$$

$$d_{ave,i} = d_{li}^{0.5} \times d_{si}^{0.5} \tag{6}$$

where $f_i$ is the percentage of soil between $d_{li}$ and $d_{si}$; $d_{ave,i}$ is the average particle diameter; and $d_{li}$ and $d_{si}$ are the larger and smaller particle diameters chosen to calculate the $d_{ave,i}$. Carrier (2003) suggested modifying Eq. (6) as

$$d_{ave,i} = d_{li}^{0.404} \times d_{si}^{0.595} \tag{7}$$

The modified $d_{ave,i}$ Eq. (7) was used to calculate the equivalent particle size $d_{eq}$ in this study.

**Table 5.** Database of critical hydraulic gradient $i_{cr}$ of soil.

| | | Soil property and test result | | | | | | Soil particle size | | | | | Internal stability criteria | | | |
|---|---|---|---|---|---|---|---|---|---|---|---|---|---|---|---|---|
| References | Test no. | $C_u$ | $C_c$ | USCS | $G_s$ | $n$ | Measured $i_{cr}$ | $d_{60}$ (mm) | $d_{20}$ (mm) | $d_{10}$ (mm) | $d_5$ (mm) | $d_{eq}$ (mm) | Kezdi (1979) $(d_{15c}/d_{85f})_{max}$ | Result | Kenney and Lau (1986) $(H/F)_{min}$ | Result |
| Skempton and Brogan (1994) | S1 | 1.85 | 1.06 | SP | 2.65 | 0.49 | 0.69 | 0.16 | 0.11 | 0.08 | 0.08 | 0.14 | 1.42 | S | >10 | S |
| | S2 | 2.63 | 1.11 | SP | 2.65 | 0.38 | 1.01 | 0.56 | 0.30 | 0.21 | 0.17 | 0.43 | 1.73 | S | 8.00 | S |
| | S3 | 3.05 | 0.87 | SP | 2.65 | 0.46 | 0.90 | 0.31 | 0.14 | 0.10 | 0.08 | 0.22 | 1.73 | S | 1.39 | S |
| | F | 1.13 | 1.01 | SP | 2.65 | 0.40 | 1.05 | 0.81 | 0.76 | 0.72 | 0.66 | 0.77 | 1.15 | S | >10 | S |
| | A | 23.46 | 9.08 | SP | 2.65 | 0.34 | 0.20 | 4.27 | 1.67 | 0.18 | 0.13 | 2.06 | 13.14 | U | 0.12 | U |
| | B | 9.05 | 3.50 | SP | 2.65 | 0.37 | 0.34 | 4.27 | 1.67 | 0.47 | 0.20 | 2.38 | 8.21 | U | 1.22 | S |
| | C | 6.46 | 2.50 | SW | 2.65 | 0.38 | 1.00 | 4.27 | 1.67 | 0.66 | 0.37 | 2.48 | 4.38 | U | 1.96 | S |
| | D | 4.17 | 1.83 | SP | 2.65 | 0.37 | 1.00 | 4.51 | 2.16 | 1.08 | 0.57 | 2.53 | 3.57 | S | 3.34 | S |
| Mörz et al. (2007) | 1 | 2.38 | 1.09 | SP | 2.65 | 0.36 | 1.13 | 0.45 | 0.26 | 0.19 | 0.15 | 0.36 | 2.30 | S | 6.36 | S |
| | 2 | 1.89 | 1.27 | SP | 2.65 | 0.41 | 1.03 | 0.34 | 0.23 | 0.18 | 0.15 | 0.29 | 1.55 | S | 9.84 | S |
| | 3 | 1.70 | 1.02 | SP | 2.65 | 0.40 | 0.96 | 0.18 | 0.12 | 0.11 | 0.15 | 0.15 | 1.76 | S | 1.83 | S |
| | 4 | 1.70 | 1.02 | SP | 2.65 | 0.41 | 1.05 | 0.18 | 0.12 | 0.11 | 0.09 | 0.15 | 1.76 | S | 1.83 | S |
| Mao, Duan, and Wu (2009) | a | 20.55 | 1.62 | SW | 2.65 | 0.36 | 0.29 | 3.78 | 0.29 | 0.18 | 0.14 | 2.81 | 5.86 | U | 0.51 | U |
| | b | 31.37 | 1.80 | GW | 2.65 | 0.33 | 0.36 | 7.04 | 0.64 | 0.22 | 0.13 | 3.95 | 4.78 | U | 0.81 | U |
| | c | 17.33 | 2.96 | GW | 2.65 | 0.33 | 0.28 | 10.13 | 2.37 | 0.58 | 0.36 | 6.06 | 6.52 | U | 0.83 | U |
| | d | 32.50 | 10.33 | GP | 2.65 | 0.32 | 0.22 | 9.31 | 2.96 | 0.29 | 0.13 | 3.82 | 21.71 | U | 0.33 | U |
| | A | 53.16 | 24.93 | GP | 2.65 | 0.31 | 0.18 | 13.97 | 0.63 | 0.26 | 0.15 | 0.93 | 16.92 | U | 0.00 | U |
| | B | 53.16 | 30.21 | GP | 2.65 | 0.31 | 0.15 | 13.97 | 0.88 | 0.26 | 0.15 | 1.44 | 24.48 | U | 0.02 | U |
| | C | 42.67 | 27.48 | GP | 2.65 | 0.31 | 0.13 | 13.97 | 10.04 | 0.33 | 0.17 | 3.66 | 34.23 | U | 0.05 | U |
| | D | 27.60 | 12.94 | GP | 2.65 | 0.28 | 0.30 | 13.97 | 1.21 | 0.51 | 0.25 | 2.23 | 9.10 | U | 0.01 | U |
| Ahlinhan and Achmus (2010) | A1-1 | 2.08 | 0.97 | SP | 2.65 | 0.50 | 0.71 | 0.2 | 0.12 | 0.09 | 0.08 | 0.16 | 1.48 | S | 6.36 | S |
| | A1-2 | | | | | 0.47 | 0.80 | | | | | | | | | |
| | A1-3 | | | | | 0.44 | 0.89 | | | | | | | | | |
| | A1-4 | | | | | 0.41 | 0.94 | | | | | | | | | |
| | A2-1 | 3.00 | 1.01 | SP | 2.65 | 0.38 | 0.90 | 0.62 | 0.29 | 0.21 | 0.15 | 0.44 | 1.86 | S | 3.18 | S |
| | A2-2 | | | | | 0.35 | 0.97 | | | | | | | | | |
| | A2-3 | | | | | 0.33 | 0.98 | | | | | | | | | |
| | E1-1 | 6.81 | 3.08 | SP | 2.65 | 0.38 | 0.31 | 1.50 | 0.84 | 0.22 | 0.15 | 0.96 | 5.45 | U | 1.13 | S |
| | E1-2 | | | | | 0.38 | 0.37 | | | | | | | | | |
| | E1-3 | | | | | 0.35 | 0.58 | | | | | | | | | |
| | E2-1 | 12.62 | 5.67 | SP | 2.65 | 0.35 | 0.18 | 1.38 | 0.73 | 0.11 | 0.08 | 0.6 | 8.96 | U | 0.31 | U |
| | E2-2 | | | | | 0.34 | 0.20 | | | | | | | | | |
| | E2-3 | | | | | 0.29 | 0.25 | | | | | | | | | |
| | E3-1 | 21.16 | 13.51 | SP | 2.65 | 0.34 | 0.18 | 2.42 | 1.54 | 0.11 | 0.08 | 1.2 | 19.11 | U | 0.00 | U |
| | E3-2 | | | | | 0.32 | 0.20 | | | | | | | | | |
| Ke and Takahashi (2011) | A-1 | 17.25 | 7.40 | SP | 2.63 | 0.39 | 0.13 | 1.79 | 0.17 | 0.10 | 0.08 | 0.55 | 9.11 | U | 0.15 | U |
| | A-2 | | | | | 0.34 | 0.21 | | | | | | | | | |
| | B-1 | 15.37 | 7.49 | SP | 2.63 | 0.41 | 0.15 | 1.79 | 0.35 | 0.12 | 0.09 | 0.73 | 10.23 | U | 0.26 | U |
| | B-2 | | | | | 0.35 | 0.23 | | | | | | | | | |
| | C-1 | 13.87 | 7.69 | SP | 2.63 | 0.40 | 0.21 | 1.79 | 1.11 | 0.13 | 0.09 | 0.94 | 11.79 | U | 0.29 | U |
| | C-2 | | | | | 0.35 | 0.24 | | | | | | | | | |
| This study | B | 1.72 | 1.01 | SP | 2.65 | 0.42 | 0.98 | 0.3 | 0.20 | 0.18 | 0.16 | 0.25 | 1.28 | S | 4.43 | S |
| | C | 1.77 | 1.03 | SP | 2.65 | 0.41 | 1.01 | 1.28 | 0.86 | 0.72 | 0.60 | 1.07 | 1.44 | S | 3.38 | S |
| | G | 12.7 | 8.82 | SP | 2.65 | 0.40 | 0.34 | 3.9 | 2.64 | 0.31 | 0.23 | 1.84 | 5.01 | U | 0.11 | U |

S, stable; U, unstable.

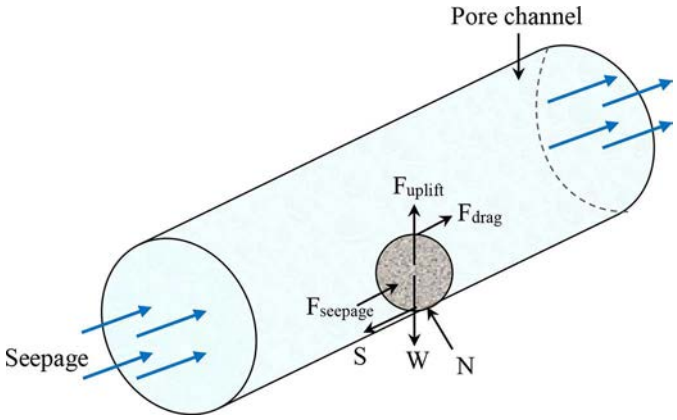


Figure 12. Illustration of forces acting on a particle in a pore channel considered in Zhou's force equilibrium model (*W*, soil particle self-weight; *N*, normal force; *S*, shear resistance; $F_{drag}$, drag force; $F_{uplift}$, uplift force; $F_{seepage}$, seepage force).

Table 6. Summary of $i_{cr}$ prediction equations.

| Reference | Formula | Background |
|---|---|---|
| Terzaghi (1929) | $i_{cr}=(G_s-1)(1-n)$ | Effective stress equals to zero |
| Wu (1980) | $i_{cr}=(G_s-1)[d_f/(d_f+e\times d_{eq})]$ | |
| Liu (1992) | $i_{cr}=2.2(G_s-1)(1-n)^2(d_5/d_{20})$ | Force equilibrium on a single soil particle |
| Zhou, Bai, and Yao (2010) | $i_{cr}=\frac{2}{3}(G_s-1)d_f^2/\left[d_f^2+\frac{\beta}{15}\frac{d_{eq}^2n^2}{(1-n)^2}\right]$ | |

$G_s$ = specific gravity; $n$ = porosity; $d_f$ = particle diameter of eroded soil caused by seepage (=$d_{10}$); $e$ = void ratio; $d_{eq}$ = equivalent particle diameter; $\beta$ = a coefficient (=3.5).

### Liu (1992)

Liu's $i_{cr}$ prediction method (Liu 1992) is based on the force equilibrium on a soil particle subject to seepage force, the weight of the soil particle, and uplift force. Liu's $i_{cr}$ equation is expressed as

$$i_{cr}=2.2(1-n)^2(G_s-1)\frac{d_5}{d_{20}} \tag{8}$$

where $G_s$ is the specific gravity of soil solids; $n$ is the porosity of soil; and $d_5$ and $d_{20}$ are the particle diameters at the finer

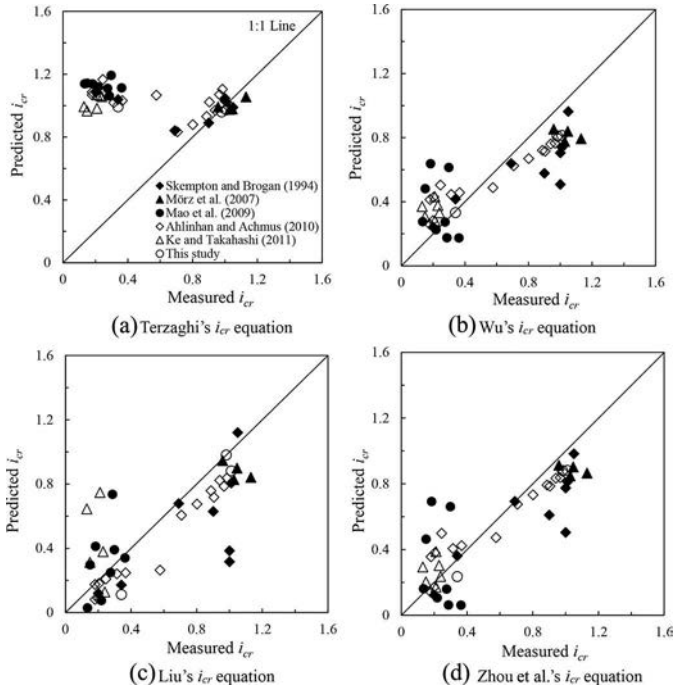


Figure 13. Overall comparison of predicted and measured critical hydraulic gradient.

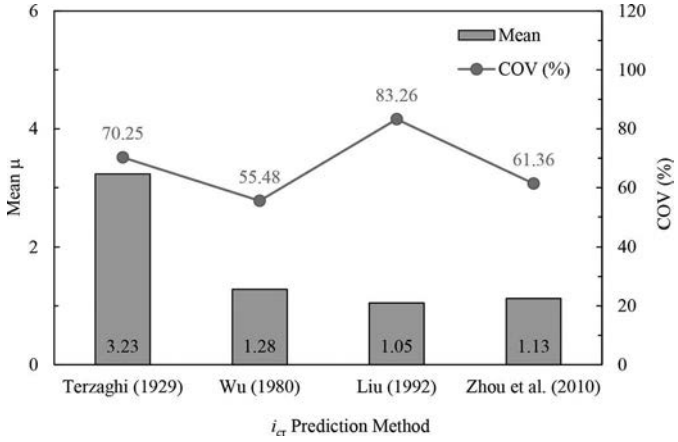


Figure 14. Statistic chart of $i_{cr}$ prediction equations under overall comparison.

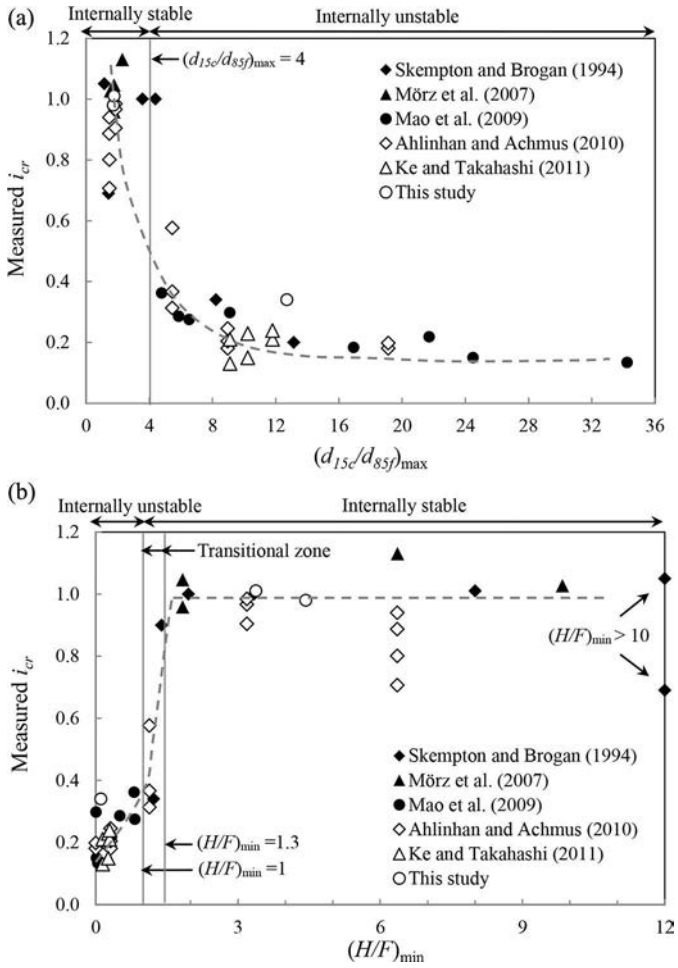


Figure 15. Variation of critical hydraulic gradients with internal stability numbers: (a) Kezdi (1979); (b) Kenney and Lau (1986).

percentage of 5 and 20% in the particle size distribution curve, respectively. The term $d_5$ represents the particle size of the eroded soil particle used in Liu's model.

### Zhou, Bai, and Yao (2010)

On the basis of Kovacs's pore channel model (Kovacs 1981); Zhou, Bai, and Yao (2010) developed a physical model for determining the critical hydraulic gradient at the onset of fine particle motion. Zhou's method considers the upward seepage force, dragging force, weight of the soil particle, uplift force, and friction force acting on the soil particle (Figure 12). Zhou's $i_{cr}$ equation is formulated as

$$i_{cr} = \frac{2}{3}(G_s - 1)\frac{{d_f}^2}{{d_f}^2 + \frac{\beta}{15}\frac{{d_{eq}}^2 n^2}{(1-n)^2}} \quad (9)$$

where $G_s$ is the specific gravity of soil solids; $n$ is the porosity of soil; $d_f$ is the eroded particle diameter ($=d_{10}$); $d_{eq}$ is the equivalent particle diameter (Eqs. 5–7); and $\beta$ is a coefficient. Zhou, Bai, and Yao (2010) suggested $\beta = 3.5$ on the basis of experimental results. A similar $i_{cr}$ prediction model was proposed by Indraratna and Radampola (2002) for examining the filtration behavior of uniform fine gravel filters retaining fine base sand.

### Overall comparison of $i_{cr}$ prediction methods

Figure 13 shows a comparison of the predicted and measured $i_{cr}$ calculated using all compiled data. Terzaghi's prediction results concentrate on $i_{cr} \approx 1$, whereas other $i_{cr}$ prediction methods generate a wider range of prediction results. To evaluate the performance of the $i_{cr}$ prediction methods quantitatively, a model factor $M$ is defined as follows:

$$M = \frac{i_{cr,p}}{i_{cr,m}} \quad (10)$$

where $i_{cr,p}$ and $i_{cr,m}$ are the predicted and measured $i_{cr}$, respectively. The mean $\mu$ and the coefficient of variation

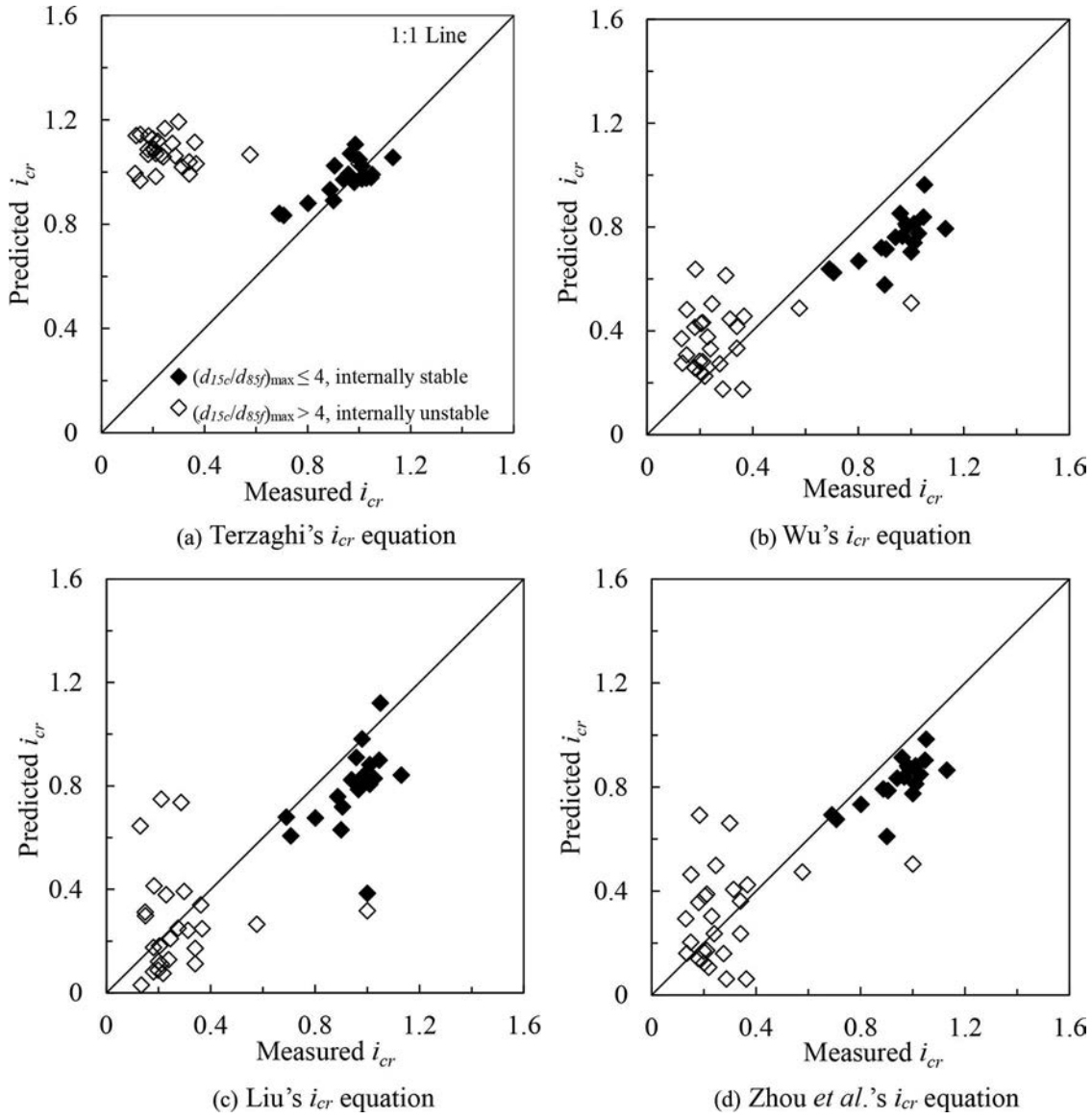


**Figure 16.** Predicted vs. measured $i_{cr}$ under Kezdi's (1979) stability criterion.

(COV) of model factor $M$ for each prediction method are calculated statistically. An ideal prediction method has a mean $\mu = 1$and COV $= 0$.

The statistical results (Figure 14) show that Terzaghi's method overestimates the measured $i_{cr}$ by up to three times ($\mu = 3.23$). Other methods have $\mu$ values close to 1.0 but unreasonably high COV values. For example, Liu's method produces the most accurate prediction result ($\mu = 1.05$) but the highest COV value (COV = 83.26%). No single prediction method performed optimally for all soil types in the overall comparison. It is because each prediction method was developed on the basis of one specialized theoretical background (i.e., $\sigma_v' = 0$ in Terzaghi's method and force equilibrium on a soil particle in Wu's, Liu's, and Zhou's methods), no prediction method is applicable to all soils.

### Comparison based on soil internal stability

In this section, the accuracy of the $i_{cr}$ prediction methods is evaluated according to the internal stability of soil determined using both Kezdi's and Kenney and Lau's internal stability criteria. The classification results (Table 5) indicate that 18 and 23 of 44 soils are classified as internally unstable by Kezdi's and Kenney and Lau's internal stability criteria, respectively. Figure 15 shows the variation of compiled $i_{cr}$ data from experimental tests with internal stability numbers. The scatter is mainly caused by the influence of porosity on $i_{cr}$, which is not considered in the selected stability criteria. The difference in the classification results between Kezdi's and Kenney and Lau's internal stability criteria is attributable to three soils (the soils used in Tests B and C in Skempton and Brogan (1994) and the soil used in Test E1 in Ahlinhan and Achmus (2010)) that have $(H/F)_{min}$ values located in the transitional area (i.e., $1.0 < (H/F)_{min} < 1.3$), as shown in Figure 15b. These soils are classified as internally stable by Kenney and Lau's criteria but classified as internally unstable by Lau's criteria.

Figures 16 and 17 show the predicted and measured $i_{cr}$ values for internally stable and unstable soils. Figure 18 summarizes the statistical results for each $i_{cr}$ prediction method according to the soil internal stability. For internally stable soils,

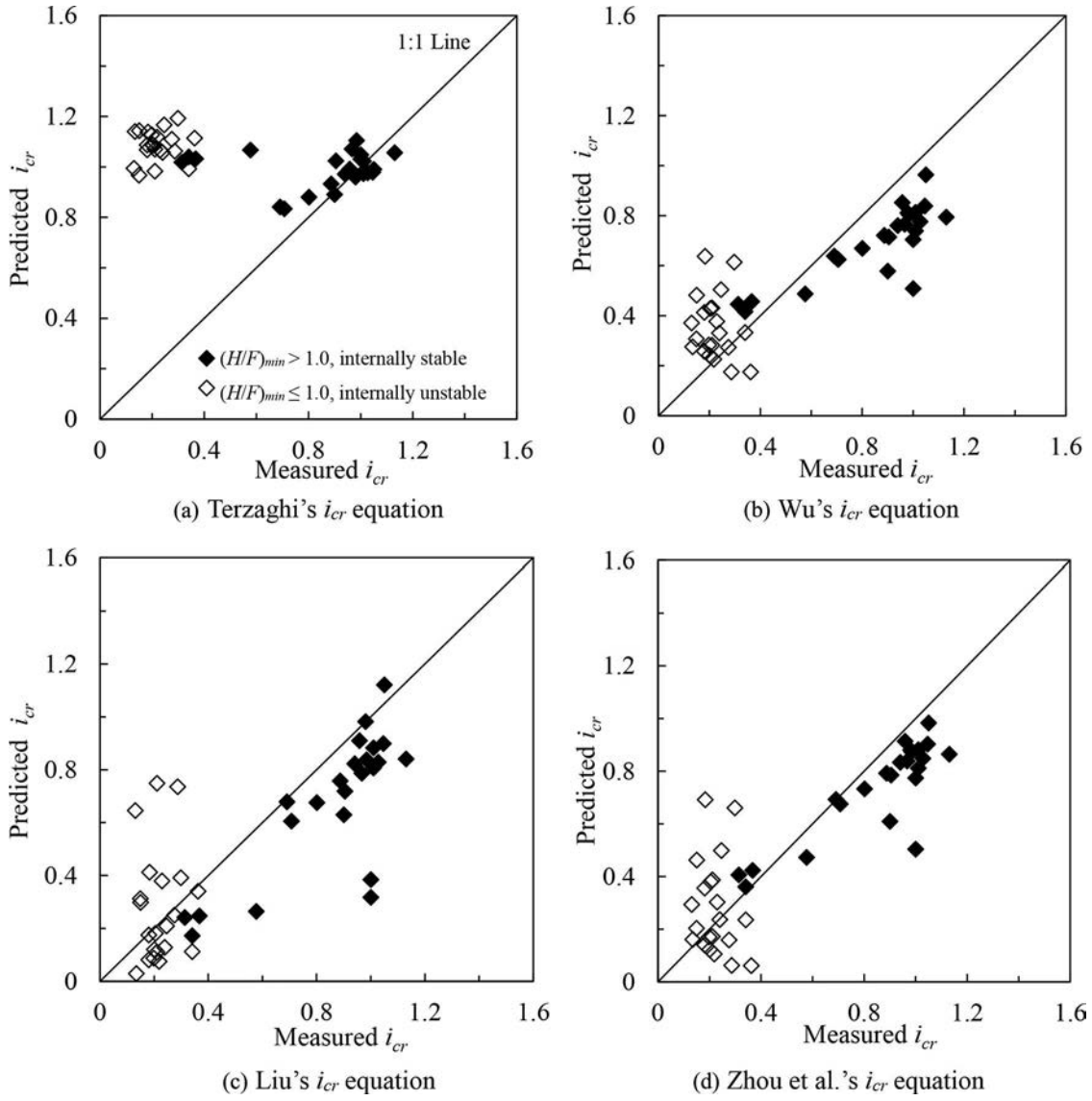


Figure 17. Predicted vs. measured $i_{cr}$ under Kenney and Lau's (1986) stability criterion.

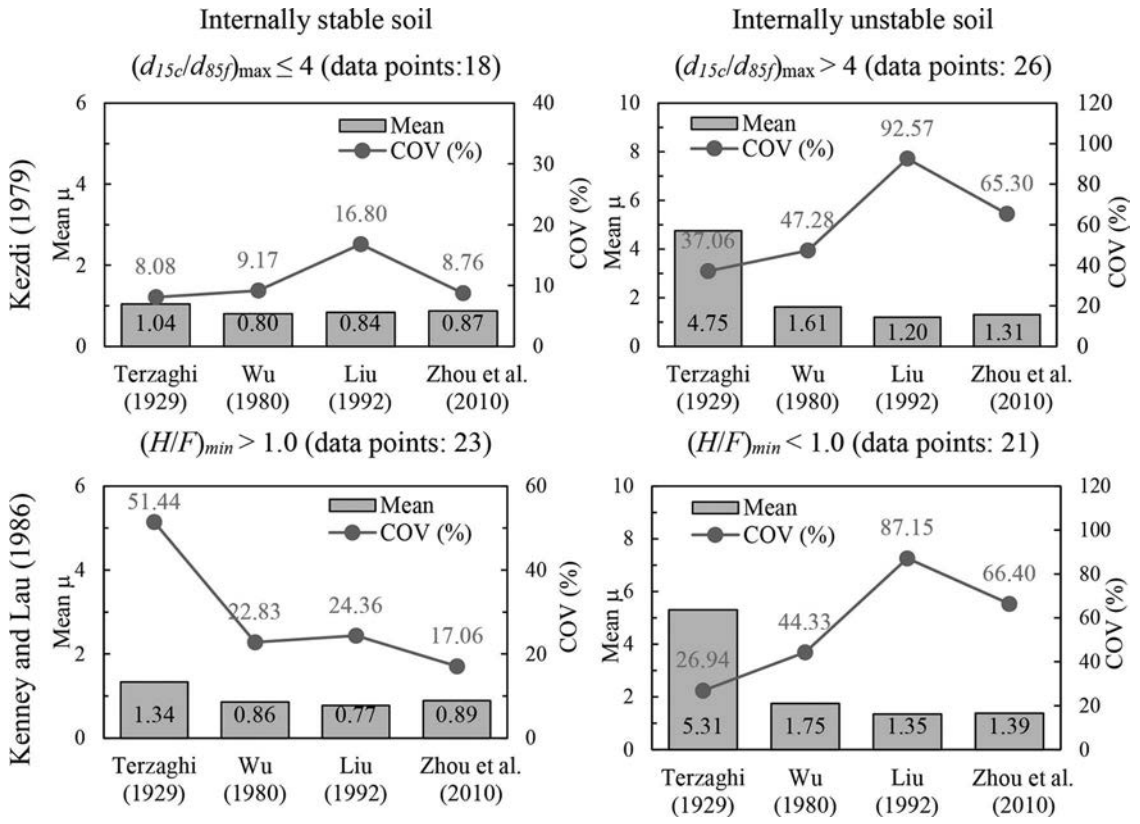


**Figure 18.** Statistic chart of $i_{cr}$ prediction equations based on stability criteria.

Terzaghi's method with Kezdi's internal stability criterion has the highest performance ($\mu = 1.04$ and COV = 8.08%). Terzaghi's method with Kenney and Lau's criterion produces a high COV value (COV = 51.44%) because there are three soils (five data points) in the transitional area, classified as internally stable by Kenney and Lau's criterion, that have $i_{cr}$ values lower than the predicted $i_{cr}$ values. Methods based on the force equilibrium on a soil particle show underestimation of the $i_{cr}$ values ($\mu < 1.0$). Zhou's method with Kezdi's criterion yields $\mu = 0.87$ with COV = 8.76%, which is more accurate than the predictions by Wu's and Liu's methods. In summary, Terzaghi's method with Kezdi's criterion shows the most accurate results with the smallest variance for predicting $i_{cr}$ for internally stable soils. The reason is that the theoretical background ($\sigma_v' = 0$) of Terzaghi's method is appropriate for the piping failure mechanism of internally stable soils.

For internally unstable soils, Tezaghi's method overestimates the $i_{cr}$ values by approximately fivefold ($\mu = 4.75$ and 5.31 according to Kezdi's and Kenney and Lau's criteria, respectively). This statistical result is in agreement with the findings from many studies that the $i_{cr}$ value can be approximately one-fifth to one-third of Terzaghi's theoretical value for internally unstable soil. Methods based on the force equilibrium on a soil particle generally produce reasonable $\mu$ values ($\mu = 1.20$ and 1.61 according to Kezdi's criterion and $\mu = 1.35$ and 1.75 according to Kenney and Lau's criteria), but the COV values are excessively high. The high COV values can be attributed to the following causes:

(1) Model uncertainty: Suffusion is a complex phenomenon, dependent upon hydraulic conditions of pore flow, soil particle shape, soil packing and arching inside the pore structures, and soil stress states. The selected prediction methods are simplified models, which may not fully address the complexity of suffusion as discussed above. In addition, the parameter $d_f$, the particle size of eroded soil, can exert a crucial influence on the $i_{cr}$ prediction. However, the value of $d_f$ is obtained on the basis of assumption (using $d_{10}$ in Wu's and Zhou's methods and $d_5$ in Liu's method). To improve the accuracy and reduce the uncertainty of the $i_{cr}$ prediction methods, the real particle sizes of eroded soils must be measured by collecting the washed-out fine particles during tests.
(2) Uncertainty in determining $i_{cr}$ for internally unstable soils: Unlike uniform sand, which exhibits an apparent turning point on its $i$–$v$ curve (i.e., measured velocity suddenly increases or hydraulic gradient decreases), the piping of internally unstable soils occurs progressively. Hence, it is difficult to determine the $i_{cr}$ value exactly corresponding to the onset of fine particle movement.

In summary, to estimate a soil's $i_{cr}$ for engineering applications, the soil's internal stability should be determined first. For soil classified as internally stable, Terzaghi's method can be used to obtain $i_{cr}$ values accurately. For soil classified as internally unstable, the selected methods based on the force equilibrium on a soil particle generally produce reasonable $\mu$ values, but the COV values are considerably high. Because the accurate prediction of $i_{cr}$ for internally unstable soil retains considerable uncertainty, conducting a few supplementary experimental tests to calibrate the input parameters of the prediction method and to validate the predicted $i_{cr}$ value is advised.

## Conclusion

An upward seepage test system was developed for investigating piping failures and the associated critical hydraulic gradients of soils with different gradations. A data set of soil test results with a wide variation of grain size distributions was compiled. Using the information in the data set, several $i_{cr}$ prediction methods were examined and their accuracies were statistically assessed and compared. Conclusions drawn from this study are presented as follows:

(1) A soil's piping failure mode and critical hydraulic gradient were influenced by the soil's gradation.
(2) The piping failures of internally stable soils (i.e., Fu-Long sand and quartz sand) were consistent with an effective stress equal to zero ($\sigma_v' = 0$). The specimens failed through either general volume expansion or the opening of a horizontal crack around or below mid-depth, which then moved upward and eventually broke through the top surface of the soil.
(3) For internally unstable soil (i.e., gap-graded sand), a piping failure occurred in the form of internal erosion of fine particles, where the fine particles in the specimen were vigorously eroded out by an upward seepage flow. The coarse particles remained stable under this hydraulic condition.
(4) The average $i_{cr}$ values of Fu-Long sand and quartz sand ($i_{cr} = 0.98$ and 1.01, respectively) are in good agreement with Terzaghi's theoretical value. The average $i_{cr}$ value of gap-graded sand ($i_{cr} = 0.34$) is far lower than Terzaghi's predicted $i_{cr}$ value.
(5) Statistical results indicated that no $i_{cr}$ prediction method selected in this study is applicable to all soils because each prediction method was developed on the basis of one specialized theoretical background and no surveyed method can effectively address different piping failure modes for soils with different gradations.
(6) For internally stable soils, the statistical results indicated that Terzaghi's method with Kezdi's internal stability criterion provides the most accurate results with the smallest variance (model bias mean $\mu = 1.04$ and COV = 8.08%).
(7) For internally unstable soils, Tezaghi's method overestimates the $i_{cr}$ values by approximately fivefold. Methods based on the force equilibrium on a soil particle generally produce reasonable $\mu$ values ($\mu = 1.20$–$1.61$ according to Kezdi's criterion and $\mu = 1.35$–$1.75$ according to Kenney and Lau's criteria), but the COV values are excessively high. The accurate prediction of $i_{cr}$ for internally unstable soil remains a considerable uncertainty.

## Nomenclature

| | |
|---|---|
| $c$ | coefficient to estimate critical shear stress $\tau_c$ (N/m$^3$) |
| $C_c$ | coefficient of gradation ($=d_{30}^2/d_{60}/d_{10}$) (dimensionless) |
| $C_u$ | uniformity coefficient ($=d_{60}/d_{10}$) (dimensionless) |
| COV | Coefficient of variation of model factor (dimensionless) |
| $d$ | arbitrary particle diameter (m) |
| $d_{15c}$ | particle size at finer percent of 15% in coarse fraction (m) |
| $d_{85f}$ | particle size at finer percent of 85% in fine fraction (m) |
| $d_{eq}$ | equivalent particle diameter (m) |
| $d_f$ | particle diameter of eroded soil (m) |
| $d_n$ | particle size at finer percent of $n$% (m) |
| $D_r$ | relative density of soil (dimensionless) |
| $F$ | finer percent at particle diameter $d$ (dimensionless) |
| $H$ | finer percent increment between $d$ and $4d$ (dimensionless) |
| $e$ | void ratio of soil (dimensionless) |
| $e_{max}$, $e_{min}$ | maximum and minimum void ratio of soil (dimensionless) |
| $k$ | hydraulic conductivity of soil (m/s) |
| $K$ | absolute hydraulic conductivity (m$^2$) |
| $M$ | model factor ($=i_{cr,p}/i_{cr,m}$) (dimensionless) |
| $n$ | porosity of soil (dimensionless) |
| $v$ | discharge velocity (m/s) |
| $i$ | hydraulic gradient (dimensionless) |
| $i_{cr}$ | critical hydraulic gradient (dimensionless) |
| $i_{cr,m}$ | measured critical hydraulic gradient (dimensionless) |
| $i_{cr,p}$ | predicted critical hydraulic gradient (dimensionless) |
| $\beta$ | coefficient (=3.5) (dimensionless) |
| $\Delta i$ | increment of applied hydraulic gradient in test (dimensionless) |
| $\eta$ | dynamic viscosity of water (N/m$^2$/s) |
| $\gamma_{sat}$ | unit weight of saturated soil (N/m$^3$) |
| $\gamma'$ | submerged unit weight of saturated soil (N/m$^3$) |
| $\gamma_w$ | unit weight of water (=9.81 kN/m$^3$) (N/m$^3$) |
| $\mu$ | mean value of model factor (dimensionless) |
| $\sigma_v'$ | vertical effective stress in soil specimen (Pa) |

## Funding

The authors gratefully acknowledge the financial support from the Ministry of Science and Technology, Taiwan with the research fund granted to the first author (NSC100-2221-E-011-0115).

## References

Adams, B. T., M. Xiao, and A. Wright. 2013. Erosion mechanisms of organic soil and bioabatement of piping erosion of sand. *Journal of Geotechnical and Geoenvironmental Engineering* 139 (8):1360–68. doi:10.1061/(asce)gt.1943-5606.0000863

Ahlinhan, M. F., and M. Achmus. 2010. Experimental investigation of critical hydraulic gradients for unstable soils. *Scour and Erosion* 599–608. doi:10.1061/41147(392)58

Bendahmane, F., D. Marot, and A. Alexis. 2008. Experimental parametric study of suffusion and backward erosion. *Journal of Geotechnical and Geoenvironmental Engineering* 134 (1):57–67. doi:10.1061/(asce)1090-0241(2008)134:1(57)

Carrier, W. D. 2003. Goodbye, Hazen; hello, Kozeny-Carman. *Journal of Geotechnical and Geoenvironmental Engineering* 129 (11):1054–56. doi:10.1061/(asce)1090-0241(2003)129:11(1054)

Chang, D. S., and L. M. Zhang. 2011a. A stress-controlled erosion apparatus for studying internal erosion in soils. *Geotechnical Testing Journal* 34 (6):579–89. doi:10.1520/GTJ103889

Chang, D. S., and L. M. Zhang. 2011b. Internal stability criteria for soils. *Rock and Soil Mechanics* 32:253–59. (in Chinese).
Chang, D. S., and L. M. Zhang. 2013a. Critical hydraulic gradients of internal erosion under complex stress states. *Journal of Geotechnical and Geoenvironmental Engineering* 139 (9):1454–67. doi:10.1061/(asce)gt.1943-5606.0000871
Chang, D. S., and L. M. Zhang. 2013b. Extended internal stability criteria for soils under seepage. *Soils and Foundations* 53 (4):569–83. doi:10.1016/j.sandf.2013.06.008
Danka, J., and L. M. Zhang. 2015. Dike failure mechanisms and breaching parameters. *Journal of Geotechnical and Geoenvironmental Engineering* 141 (9):04015039. doi:10.1061/(asce)gt.1943-5606.0001335
Fannin, J. 2008. Karl Terzaghi: From theory to practice in geotechnical filter design. *Journal of Geotechnical and Geoenvironmental Engineering* 134:267–76. doi:10.1061/(asce)1090-0241(2008)134:3(267)
Fell, R., and J. J. Fry. 2013. State of the art on the likelihood of internal erosion of dams and levees by means of testing. In *Erosion in geomechanics applied to dams and levees*, ed. by S. Bonelli Chapter 1, 1–99. London, UK: ISTE-Wiley.
Fell, R., C. F. Wan, J. Cyganiewicz, and M. Foster. 2003. Time for development of internal erosion and piping in embankment dams. *Journal of Geotechnical and Geoenvironmental Engineering* 129 (4):307–14. doi:10.1061/(ASCE)1090-0241(2003)129:4(307)
Fleshman, M. S., and J. D. Rice. 2014. Laboratory modeling of the mechanisms of piping erosion initiation. *Journal of Geotechnical and Geoenvironmental Engineering* 140 (6):04014017. doi:10.1061/(asce)gt.1943-5606.0001106
Fry, J. J. 2012. Introduction to the process of internal erosion in hydraulic structures: Embankment dams and dikes. In *Erosion of geomaterials*, ed. by S. Bonelli Chapter 1, 1–36. London, UK: ISTE-Wiley.
Garner, S. J., and R. J. Fannin. 2010. Understanding internal erosion: A decade of research following a sinkhole event. *The International Journal on Hydropower and Dams* 17 (3):93–98.
Hagerty, D. J. 1991a. Piping/sapping erosion. I: Basic considerations. *Journal of Hydraulic Engineering* 117 (8):991–1008. doi:10.1061/(asce)0733-9429(1991)117:8(991)
Hagerty, D. J. 1991b. Piping/sapping erosion. II: Identification-diagnosis. *Journal of Hydraulic Engineering* 117 (8):1009–25. doi:10.1061/(asce)0733-9429(1991)117:8(1009)
Huang, W. C., M. C. Weng, and R. K. Chen. 2014. Levee failure mechanisms under the extreme rainfall event – A case study in southern Taiwan. *Natural Hazards* 70:1287–307. doi:10.1007/s11069-013-0874-9
Indraratna, B., V. T. Nguyen, and C. Rujikiatkamjorn. 2011. Assessing the potential of internal erosion and suffusion of granular soils. *Journal of Geotechnical and Geoenvironmental Engineering* 137 (5):550–54. doi:10.1061/(asce)gt.1943-5606.0000447
Indraratna, B., and S. Radampola. 2002. Analysis of critical hydraulic gradient for particle movement in filtration. *Journal of Geotechnical and Geoenvironmental Engineering* 128 (4):347–50. doi:10.1061/(asce)1090-0241(2002)128:4(347)
Istomina, V. S. 1957. *Filtration stability of soils*. Moscow: Gostroizdat.
Ke, L., and A. Takahashi. 2011. Strength reduction of gap-graded cohesionless soil due to internal erosion. *Unsaturated Soils: Theory and Practice* 203–8.
Ke, L. and A. Takahashi. 2012. Strength reduction of cohesionless soil due to internal erosion induced by one-dimensional upward seepage flow. *Soils and Foundations* 52(4): 698–711. doi:10.1016/j.sandf.2012.07.010
Ke, L., and A. Takahashi. 2014. Experiment investigations on suffusion characteristics and its mechanical consequences on saturated cohesionless soil. *Soils and Foundations* 54 (4):713–30. doi:10.1016/j.sandf.2014.06.024
Kenney, T. C., and D. Lau. 1985. Internal stability of granular filters. *Canadian Geotechnical Journal* 22:245–25. doi:10.1139/t85-029
Kenney, T. C., and D. Lau. 1986. Internal stability of granular filters: Reply. *Canadian Geotechnical Journal* 23:420–23. doi:10.1139/t86-068
Kezdi, A. 1979. *Soil physics: Selection topics (developments in geotechnical engineering)*. Amsterdam, Netherlands: Elsevier Science Ltd.
Khilar, K. C., H. S. Folger, and D. H. Gray. 1985. Model for piping plugging in earthen structures. *Journal of Geotechnical Engineering* 111 (7):833–46. doi:10.1061/(asce)0733-9410(1985)111:7(833)
Kovacs, G. 1981. *Seepage hydraulics*, 730. Amsterdam: Elsevier Scientific Publishing Company.
Li, M., and R. J. Fannin. 2008. Comparison of two criteria for internal stability of granular soil. *Canadian Geotechnical Journal* 45 (9):1303–09. doi:10.1139/t08-046
Li, M., and R. J. Fannin. 2012. A theoretical envelope for internal stability of cohesionless soil. *Geotechnique* 62 (1):77–80. doi:10.1680/geot.10.t.019
Li, M., and R. J. Fannin. 2013. Capillary tube model for internal stability of cohesionless soil. *Journal of Geotechnical and Geoenvironmental Engineering* 139 (5):831–34. doi:10.1061/(asce)gt.1943-5606.0000790
Liu, J. 1992. *Seepage stability and seepage control of soil*. Beijing, China: Water Resources and Electric Power Press.
Mao, C. X. 2005. Study on piping a filters: Part1 of piping. *Rock and Soil Mechanics* 26 (2):209–15. (in Chinese).
Mao, C. X., X. B. Duan, and L. J. Wu. 2009. Study of critical gradient of piping for various gran sizes in sandy gravels. *Rock and Soil Mechanics* 30 (12):3705–09. (in Chinese).
Moffat, R., and R. J. Fannin. 2011a. Spatial and temporal progression of internal erosion in cohesionless soil. *Canadian Geotechnical Journal* 48 (3):399–412. doi:10.1139/t10-071
Moffat, R., and R. J. Fannin. 2011b. A hydromechanical relation governing internal stability of cohesionless soil. *Canadian Geotechnical Journal* 48 (3):413–24. doi:10.1139/t10-070
Moffat, R., and P. Herrera. 2015. Hydromechanical model for internal erosion and its relationship with the stress transmitted by the finer soil fraction. *Acta Geotechnica* 10:643–50. doi:10.1007/211440-014-0326-z
Mörz, T., E. A. Karlik, S. Kreiter, and A. Kopf. 2007. An experimental setup for fluid venting in unconsolidated sediments: New insights to fluid mechanics and structures. *Sedimentary Geology* 196:251–67. doi:10.1016/j.sedgeo.2006.07.006
Nichols, R. J., R. S. J. Sparks, and C. J. N. Wilson. 1994. Experimental studies of the fluidization of layered sediments and the formation of fluid escape structures. *Sedimentology* 41:233–53. doi:10.1111/j.1365-3091.1994.tb01403.x
Ojha, C. S. P., V. P. Singh, and D. D. Adrian. 2003. Determination of critical head in soil piping. *Journal of Hydraulic Engineering* 127 (7):511–18. doi:10.1061/(asce)0733-9429(2003)129:7(511)
Parekh, M. L., W. Kanning, C. Bocovich, M. A. Mooney, and A. R. Koelewijn. 2016. Backward erosion monitored by spatial-temporal pore pressure changes during field experiments. *Journal of Geotechnical and Geoenvironmental Engineering* 04016050. doi:10.1061/(ASCE)GT.1943-5606.0001528
Peng, M., and L. M. Zhang. 2012. Breaching parameters of landslide dams. *Landslides* 9 (1):13–31. doi:10.1007/s10346-011-0271-y
Rice, J. D., and J. M. Duncan. 2010. Findings of case histories on the long-term performance of seepage barriers in dams. *Journal of Geotechnical and Geoenvironmental Engineering* 136 (1):2–15. doi:10.1061/(asce)gt.1943-5606.0000175
Rice, J. D., J. M. Duncan, and R. R. Davidson. 2007. Identification of failure mechanisms associated with seepage barriers in dams. *Embankment, Dams, and Slopes* 1–11. doi:10.1061/40905(224)2
Richards, K. S., and K. R. Reddy. 2007. Critical appraisal of piping phenomena in earth dams. *Bulletin of Engineering Geology and Environment* 66:381–402. doi:10.1007/s10064-007-0095-0
Sharif, Y. A., M. Elkholy, M. H. Chaudhry, and J. Imran. 2015. Experimental study on the piping erosion process in earthen embankments. *Journal of Hydraulic Engineering* 141 (7):04015012. doi:10.1061/(asce)hy.1943-7900.0001019
Skempton, A. W., and J. M. Brogan. 1994. Experiments on piping in sandy gravels. *Geotechnique* 44 (3):449–60. doi:10.1680/geot.1994.44.3.449
Skempton, A. W., and J. M. Brogan. 1995. Discussion on experiments on piping in sandy gravels. *Geotechnique* 45 (3):565–67. doi:10.1680/geot.1995.45.3.565
Terzaghi, K. 1943. *Theoretical soil mechanics*. New York: Wiley.
Wan, C. F., and R. Fell. 2008. Assessing the potential of internal instability and suffusion in embankment dams and their foundations. *Journal of*

*Geotechnical and Geoenvironmental Engineering* 134 (3):401–07. doi:10.1061/(asce)1090-0241(2008)134:3(401)

Wu, L. J. 1980. Calculation of critical hydraulic gradient for piping in cohesionless soils. *Hydro-Science and Engineering* 4:90–95. (in Chinese).

Xu, Y., and L. Zhang. 2009. Breaching parameters of earth and rock fill dams. *Journal of Geotechnical and Geoenvironmental Engineering* 135 (12):1957–70. doi:10.1061/(ASCE)GT.1943-5606.0000162

Zhang, L. M., Y. Xu, and J. S. Jia. 2009. Analysis of earth dam failures: A database approach. *Georisk: Assessment and Management of Risk for Engineered Systems and Geohazards* 3 (3):184–89. doi:10.1080/17499510902831759

Zhou, J., Y. F. Bai, and Z. X. Yao. 2010. A mathematical model for determination of the critical hydraulic gradient in soil piping. *Geoenvironmental Engineering and Geotechnics* 239–44. doi:10.1061/41105(378)33